Articles

Synthesis, Structural, and Theoretical Analysis of $Ru_4(CO)_{12}(\mu\text{-}PF_2)(\mu_4\text{-}P)$: Is the μ_4-P Atom a Three-Electron or a Five-Electron Donor?

Samia Kahlal,[†] Weibin Wang,[‡] Ludmila Scoles,[‡] Konstantin A. Udachin,[‡] Jean-Yves Saillard,*[,†] and Arthur J. Carty*[,‡]

LCSIM UMR-CNRS 6511, Université de Rennes 1, 35042 Rennes Cedex, France, and Steacie Institute for Molecular Sciences, National Research Council, 100 Sussex Drive, Ottawa, Canada K1A OR6

Received April 30, 2001

The X-ray molecular structure of $Ru_4(CO)_{12}(\mu\text{-}PF_2)(\mu_4\text{-}P)$ exhibits a rather open Ru_4 butterfly with no Ru−Ru bond along the butterfly hinge, which is bridged by a μ-PF_2 ligand. The μ_4-P atom unsymmetrically bridges the Ru_4 butterfly with two very different Ru−P−Ru angles: 148.71(15) and 95.43(10)°. The peculiar coordination mode of the μ_4-P atom raises the question of how many electrons (three or five) it gives to the metal framework. DFT calculations on the $[Ru_4(CO)_{12}(\mu\text{-}PF_2)(\mu_4\text{-}P)]^{2-/0/2+}$ series indicate that the phosphorus atom is better described as being a three-electron donor. Its unexpected pyramidalization is the result of atomic size and of the pinch effect of the μ-PF_2 ligand. The bonding in this cluster has been analyzed and compared to that of the related series $[Ru_4(CO)_{12}(\mu\text{-}PF_2)(\mu_4\text{-}N)]^{0/2+}$ and the $[M_4(CO)_{12}(\mu_4\text{-}E)]^{-/3-}$ (M = Fe, Ru; E = N, P). A very good agreement between the optimized geometries and the available X-ray data is observed.

Introduction

The bonding within transition-metal clusters is now well understood, mainly due to the development during the last two decades of what is generally called the polyhedral skeletal electron pair (PSEP) theory or the Wade−Mingos rules.[1] The PSEP theory correlates the cluster structure with its number of electrons. The skeletal geometries of most carbonyl clusters are shown to derive from those of deltahedra. All of the atoms constituting the cluster cage are located at the vertices of a deltahedron, but all of the vertices of the deltahedra are not necessarily unoccupied. The *closo*, *nido*, *arachno*, *hypho*... terminology applies for deltahedra having 0, 1, 2, 3... unoccupied vertices, respectively. The cluster closed-shell electron count depends on the number of vertices of the fundamental deltahedron, regardless of whether they are occupied or not. In general, the number of skeletal electron pairs (SEP), i.e. electron pairs mainly located on the cluster skeleton, is equal to the total number of vertices of the deltahedron plus 1. This rule applies also for mixed transition-metal/main-group clusters in which main-group atoms occupy vertices in the same manner as transition metals. In these clusters, each of the metallic (ML_n) or main-group (E or ER) fragments constituting the cluster cage participate in the cluster bonding by providing three orbitals for cluster bonding. The other M or E orbitals are used for M−L or E−R bonding or for holding peripheral lone pairs. An example of a mixed transition-metal/main-group cluster is the *nido* 7-SEP compound $Os_5(CO)_{15}(\mu_4\text{-}S)$,[2] sketched in Figure 1. In this cluster, the S atom retains one exo-skeletal lone pair and therefore contributes to the SEP count with four electrons.

Main-group atoms can also be found occupying interstitial positions at the center of the fundamental deltahedron of a cluster.[1,3] In the case of *closo* clusters it is fully encapsulated in the cluster cage, whereas in the case of *nido*, *arachno*, or *hypho* species, it is described as occupying an exposed position. Some examples of *closo*, *nido*, and *arachno* 7-SEP clusters exhibiting encapsulated or exposed carbon atoms[4−6] are sketched in Figure 1. The reactivity of exposed main-group atoms has been extensively investigated and compared to that of solid-state surfaces which present similar coordina-

[†] Université de Rennes 1.
[‡] National Research Council.

(1) See for example: (a) Wade, K. In *Transition Metal Clusters*; Johnson, B. F. G., Ed.; Wiley: New York, 1980; p 193. (b) Mingos, D. M. P.; Wales, D. J. *Introduction to Cluster Chemistry*; Prentice-Hall: Englewood Cliffs, NJ, 1990.

(2) Adams, R. D.; Horvàth, I. T.; Segmüller, B. E.; Yang, L.-W. *Organometallics* **1983**, *2*, 1301.

(3) Halet, J.-F. In *Topics in Physical Organometallic Chemistry*; Gielen, M. F., Ed.; Freund: London, 1992; Vol. 4, p 221.

(4) Churchill, M. R.; Wormold, J.; Knight, J.; Mays, M. J. *J. Am. Chem. Soc.* **1971**, *93*, 3073.

(5) Braye, E. H.; Dahl, L. F.; Hübel, W.; Wampler, D. L. *J. Am. Chem. Soc.* **1962**, *84*, 4633.

(6) (a) Holt, E. M.; Whitmire, K. H.; Shriver, D. F. *J. Organomet. Chem.* **1981**, *213*, 125. (b) Boeheme, R. F.; Coppens, P. *Acta Crystallogr.* **1981**, *B37*, 1914. (c) Davies, J. H.; Beno, M. A.; Williams, J. A.; Zimmie, J.; Tachikawa, M.; Muetterties, E. L. *Proc. Natl. Acad. Sci. U.S.A.* **1981**, *78*, 668.

10.1021/om010352u CCC: $20.00
Publication on Web 09/22/2001

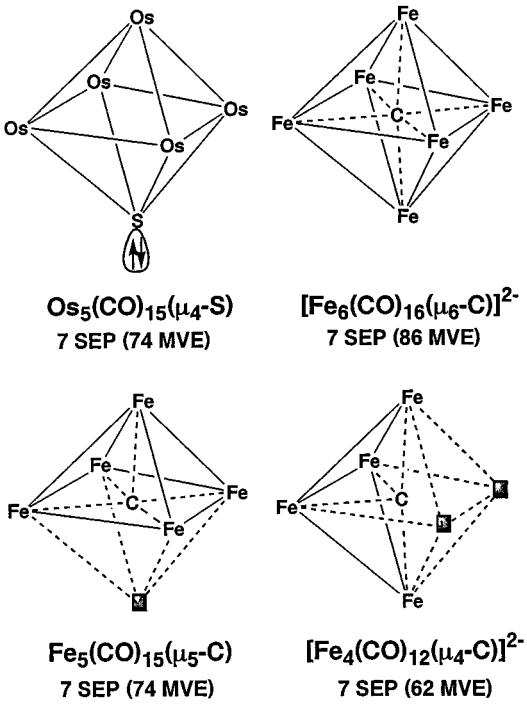

Figure 1. Examples of 7-SEP organometallic clusters in which main-group atoms occupy a vertex of the fundamental polyhedron[2] or the center of fundamental polyhedron, occupying encapsulated[4] or exposed[5,6] locations. The metal valence electron (MVE) count of the cluster can be obtained by adding the metal-based peripheral ligands and d-type nonbonding electrons to the SEP count.

tion modes of main-group atoms.[3,7] The presence of such an interstitial atom does not change the favorable closed-shell SEP count of the cluster, which remains equal to the total number of vertices of the deltahedron plus 1. Since all of the atomic orbitals of the interstitial atom are involved in cluster bonding, all of its electrons have to be counted as contributing to the total SEP count of the cluster.

Thus, transition-metal clusters can incorporate bare main-group E atoms in two ways. (i) E occupies a vertex of the skeleton of the fundamental polyhedron. It is pyramidalized and can be described as being sp^3-hybridized with the exo-skeletal hybrid containing a lone pair and the three other hybrids participating with their electrons in the skeletal bonding. (ii) E is situated at the center or within the fundamental polyhedron describing the cluster, its bonding mode being related to that of hypervalent atoms in main-group chemistry. In this case all four AO's, and consequently all of the valence electrons of E, are involved in skeletal bonding. From this point of view, it is interesting to note that the formal addition of two electrons to an M_5E cluster (isoelectronic and isostructural with $Fe_5(CO)_{15}(\mu_5\text{-}C)$,[5] for example) should result in a translation of E out of the middle of the M_4 square face toward a vertex position of the somewhat irregular fundamental octahedron, generating a structure related to that of $Os_5(CO)_{15}(\mu_4\text{-}S)$[2] (see Figure 1).[8] In principle, instability can be anticipated from the PSEP rules for closed-shell clusters exhibiting E atoms occupying a position intermediate between cases i and ii. The title compound $Ru_4(CO)_{12}(\mu\text{-}PF_2)(\mu_4\text{-}P)$ is the first clear and simple example of such an intermediate situation. We now describe its synthesis and molecular geometry and provide a rationalization of the bonding in this unexpected structure.

Experimental Section

General Considerations. The reaction was carried out under an atmosphere of nitrogen. Hexane and CH_2Cl_2 were appropriately dried prior to use. The compound $[Ru_4(CO)_{12}(\mu_4\text{-}PNEt_2)_2]$ was synthesized by the known procedure.[9]

IR spectra were recorded on a Bio-Rad FTS-40A FTIR spectrometer. The ^1H and ^{31}P NMR spectra were obtained on a Bruker DRX-400 spectrometer and ^{19}F NMR spectra on a Bruker AMX 500 MHz instrument. Elemental analyses were performed by Ms. Ann Webb of the Institute of Biological Sciences at the National Research Council of Canada.

Synthesis and Spectroscopic Characterization of $Ru_4(CO)_{12}(\mu\text{-}PF_2)(\mu_4\text{-}P)$. The cluster $[Ru_4(CO)_{12}(\mu_4\text{-}PNEt_2)_2]$ (100 mg, 0.106 mmol) was placed into a Schlenk tube and dissolved in 10 mL of CH_2Cl_2. The deep red-orange solution was thoroughly degassed and treated with an excess of $HBF_4{\cdot}OEt_2$ (54% solution, 50 μL, 0.672 mmol), resulting in an immediate lightening of the color. The reaction mixture was stirred at room temperature for 24 h; then the solvent was removed in vacuo and the oily residue was extracted with hexane. The only isolable product, $Ru_4(CO)_{12}(\mu_2\text{-}PF_2)(\mu_4\text{-}P)$ (30 mg, 30%), was obtained by recrystallization from CH_2Cl_2/hexane at −28 °C over several days. Spectral data for $Ru_4(CO)_{12}(\mu_2\text{-}PF_2)(\mu_4\text{-}P)$: IR ($CH_2Cl_2$): ν(CO) 2076 m, 2068 vs, 2039 m, 2004 w cm^{-1}. ^{31}P NMR (δ, $CDCl_3$): 671.9 (s), 249.5 (t, J_{PF} = 1142 Hz). ^{19}F NMR (δ, $CDCl_3$): −33.31 (d, J_{PF} = 1143 Hz). Anal. Calcd for $Ru_4P_2F_2O_{12}C_{12}$: C, 17.15; H, 0; N, 0. Found C, 16.93; H, 0; N, 0.

The carbonyl region of the infrared spectrum resembles that of the precursor $[Ru_4(CO)_{12}(\mu_4\text{-}PNEt_2)_2]$, but with the ν(CO) bands shifted to higher frequency. A ^1H NMR experiment failed to reveal any proton resonances. A ^{31}P NMR spectrum revealed the presence of two inequivalent phosphorus nuclei as a singlet at δ 671.9 and a triplet at δ 249.5 with a large coupling of J = 1142 Hz typical of a one-bond P−F coupling.

X-ray Analysis. A suitable crystal of dimensions 0.3 × 0.25 × 0.2 mm obtained from CH_2Cl_2/hexane was mounted on a glass fiber with 5 min epoxy cement for X-ray analysis. Intensity data were collected within the 2θ range of 1.29−28.7° using graphite-monochromated Mo Kα radiation on a Siemens SMART CCD diffractometer. Crystal and intensity data are given in Table 1. The structure was solved and refined using Patterson, Fourier, and full-matrix least-squares methods with the SHELXTL program package. All atoms were refined anisotropically to R and R_w values of 0.044 and 0.120 on the basis of 3622 unique reflections. The largest peak in the difference Fourier map was 1.30 e $Å^{-3}$. Scattering factors used, including corrections for anomalous dispersion, were taken from ref 10. A selection of bond lengths and angles is given in Table 2. All other X-ray parameters are included as Supporting Information.

(7) (a) Muetterties, E. L. *Chem. Rev.* **1979**, *79*, 91. (b) Muetterties, E. L. *Prog. Inorg. Chem.* **1981**, *28*, 203. (c) Wijeyesekara, S. D.; Hoffmann, R.; Wilker, C. N. *Organometallics* **1984**, *3*, 962.

(8) Halet, J.-F.; Saillard, J.-Y.; Lissilllour, R.; McGlinchey, M. J.; Jaouen, G. *Organometallics* **1986**, *5*, 139.

(9) (a) Kahlal, S.; Udachin, K. A.; Scoles, L.; Carty, A. J.; Saillard, J.-Y. *Organometallics* **2000**, *19*, 2251. (b) Wang, W.; Corrigan, J. F.; Enright, G. D.; Taylor, N. J.; Carty, A. J. *Organometallics* **1998**, *17*, 427. (c) Wang, W.; Carty, A. J. *New J. Chem.* **1997**, *21*, 773. (d) Yamamoto, J. H.; Udachin, K. A.; Enright, G. D.; Carty, A. J. *Chem. Commun.* **1998**, 2259.

(10) (a) *International Tables for X-ray Crystallography*; Kynoch: Birmingham, U.K., 1975; Vol. IV, Table 2.2B, pp 99−101. (b) *International Tables for X-ray Crystallography*; Kynoch: Birmingham, U.K., 1975; Vol. IV, Table 2.3.1, pp 149−150.

Table 1. Crystal Data and Structure Refinement Details for $Ru_4(CO)_{12}(\mu\text{-}PF_2)(\mu_4\text{-}P)$

empirical formula	$C_{12}F_2O_{12}P_2Ru_4$
fw	840.34
temp (K)	173(2)
wavelength (Å)	0.710 70
cryst syst	monoclinic
space group	*Pn*
a (Å)	7.0669(5)
b (Å)	15.8404(10)
c (Å)	9.7152(6)
α (deg)	90
β (deg)	100.5810
γ (deg)	90
V (Å^3)	1069.05(12)
Z	2
D_{calcd} (g cm^{-3})	2.611
abs coeff (mm^{-1})	2.995
F(000)	784
cryst size (mm)	0.3 × 0.25 × 0.2
θ range for data collection (deg)	1.29−28.70
index ranges	$-9 \le h \le 9$, $-21 \le k \le 21$, $-5 \le l \le 13$
no. of rflns collected/unique	6344/3622 (*R*(int) = 0.0873)
completeness to $2\theta = 28.70$ (%)	98.5
refinement method	full-matrix least-squares on F^2
no. of data/restraints/params	3622/2/289
goodness of fit on F^2	1.097
final *R* indices ($I > 2\sigma(I)$)	R1 = 0.0435, wR2 = 0.1196
R indices (all data)	R1 = 0.0507, wR2 = 0.1298
absolute struct param	0.12(8)
largest diff peak and hole (e Å^{-3})	1.302 and −1.715

Table 2. Summary of Important Bond Lengths (Å) and Angles (deg) for $Ru_4(CO)_{12}(\mu\text{-}PF_2)(\mu_4\text{-}P)$

Ru(1)−P(1)	2.280(3)	Ru(1)−Ru(3)	2.9878(13)
Ru(1)−P(2)	2.458(3)	Ru(1)−Ru(4)	2.9694(11)
Ru(2)−P(1)	2.274(3)	Ru(2)−Ru(3)	2.9736(11)
Ru(2)−P(2)	2.454(3)	Ru(2)−Ru(4)	2.9813(11)
Ru(3)−P(2)	2.188(3)	P(1)−F(1)	1.601(8)
Ru(4)−P(2)	2.187(3)	P(1)−F(2)	1.595(7)

P(1)−Ru(1)−P(2)	79.24(10)	Ru(2)−Ru(3)−Ru(1)	75.13(3)
P(1)−Ru(2)−P(2)	79.43(10)	Ru(3)−Ru(2)−Ru(4)	90.05(3)
P(1)−Ru(1)−Ru(4)	74.66(8)	Ru(4)−Ru(1)−Ru(3)	90.01(3)
P(1)−Ru(1)−Ru(3)	73.68(8)	F(1)−P(1)−Ru(1)	115.1(3)
P(1)−Ru(2)−Ru(3)	74.04(8)	F(1)−P(1)−Ru(2)	114.1(3)
P(1)−Ru(2)−Ru(4)	74.48(8)	F(2)−P(1)−Ru(1)	114.9(3)
P(2)−Ru(1)−Ru(3)	46.12(7)	F(2)−P(1)−Ru(2)	114.4(3)
P(2)−Ru(1)−Ru(4)	46.34(7)	F(2)−P(1)−F(1)	92.5(4)
P(2)−Ru(2)−Ru(3)	46.33(7)	Ru(2)−P(1)−Ru(1)	105.90(12)
P(2)−Ru(2)−Ru(4)	46.19(7)	Ru(2)−P(2)−Ru(1)	95.43(10)
P(2)−Ru(3)−Ru(1)	54.08(8)	Ru(3)−P(2)−Ru(1)	79.80(9)
P(2)−Ru(3)−Ru(2)	54.23(7)	Ru(3)−P(2)−Ru(2)	79.43(9)
P(2)−Ru(4)−Ru(1)	54.43(8)	Ru(4)−P(2)−Ru(1)	79.23(10)
P(2)−Ru(4)−Ru(2)	54.10(7)	Ru(4)−P(2)−Ru(2)	79.71(9)
Ru(1)−Ru(4)−Ru(2)	75.29(3)	Ru(4)−P(2)−Ru(3)	148.71(15)

Computational Details. DFT calculations[11] were carried out using the Amsterdam Density Functional (ADF) program.[12] Electron correlation was treated within the local density approximation in the Vosko−Nusair parametrization (LDA).[13] The numerical integration procedure applied for the calculations was developed by te Velde et al.[11d] A triple-ζ Slater-type orbital (STO) basis set was used for Fe 3d and 4s and for Rh and Ru 4d and 5s. A single-ζ STO was used for Fe 4p and for Rh and Ru 5p. A double-ζ STO basis set was employed for H 1s, C, N, O, and F 2s and 2p, and P 3s and 3p, extended with a single-ζ polarization function 2p for H and 3d for C, N, O, F, and P. The frozen-core approximation was used to treat the core electrons.[11a]

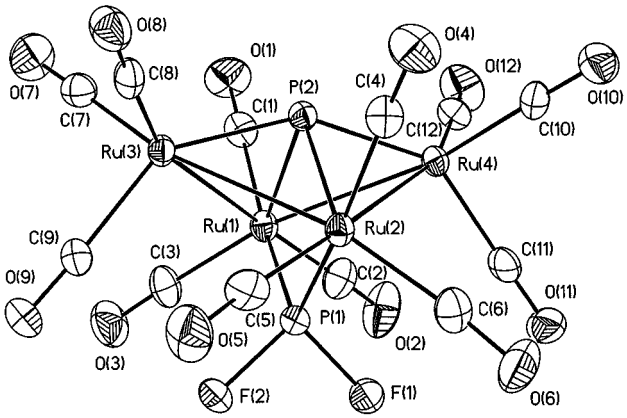

Figure 2. Crystal structure of $Ru_4(CO)_{12}(\mu\text{-}PF_2)(\mu_4\text{-}P)$.

Results and Discussion

The reaction of $[Ru_4(CO)_{12}(\mu_4\text{-}PNEt_2)_2]$ with $HBF_4 \cdot OEt_2$ was carried out with the intention of preparing the bis(fluorophosphinidene) cluster $[Ru_4(CO)_{12}(\mu_4\text{-}PF)_2]$, which by analogy with synthetic strategies developed in this laboratory,[9b−d] would provide access to the bis(phosphorus monoxide) cluster anion $[Ru_4(CO)_{12}(PO)_2]^{2-}$. It was therefore a complete surprise that the product was not the bis(phosphinidene) but its isomer, the unsymmetrical cluster $Ru_4(CO)_{12}(\mu\text{-}PF_2)(\mu_4\text{-}P)$. The same compound was subsequently obtained in similar yields from the reaction of $[Ru_4(CO)_{12}(\mu_4\text{-}PN^iPr_2)_2]$ with $HBF_4 \cdot OEt_2$, indicating that the formation of $Ru_4(CO)_{12}(\mu\text{-}PF_2)(\mu_4\text{-}P)$ is not limited to a single precursor nor is it an artifact of reaction conditions.

Structural Analysis of $Ru_4(CO)_{12}(\mu\text{-}PF_2)(\mu_4\text{-}P)$. A view of the X-ray molecular structure of $Ru_4(CO)_{12}(\mu\text{-}PF_2)(\mu_4\text{-}P)$ is shown in Figure 2. It has approximate C_{2v} symmetry. Major metrical data are given in Table 2. The four Ru atoms form a rather open butterfly, the angle between the Ru(1)Ru(2)Ru(3) and Ru(1)Ru(2)Ru(4) wings being 126°. There is no bond along the butterfly hinge (Ru(1)···Ru(2) = 3.634 (1) Å). The four Ru−Ru bond distances lie in the range 2.9694(11)−2.9878(13) Å, which is at the high end of the spectrum of values found in "electron precise" ruthenium clusters.[14] The μ_2-PF_2 ligand bridges the nonbonding Ru(1)···Ru(2) vector. The μ_4-P atom, on the other hand, unsymmetrically bridges the four Ru atoms in the butterfly with Ru(1)−P(2) and Ru(2)−P(2) distances (average 2.456 Å) significantly longer than the Ru(3)−P(2) and Ru(4)−P(2) bond lengths (average 2.188 Å). While elongated, the Ru(1)−P(2) and Ru(2)−P(2) distances are, however, still considerably shorter than the two very long Ru−P contacts in the formally 64e clusters $[Ru_4(CO)_{12}(\mu_4\text{-}P(NR_2)_2]$, where the phosphinidene ligands approach a μ_2-bonding mode. An additional feature of interest is the Ru−P(2)−Ru bond angles, with Ru(1)−P(2)−Ru(2) nearly acute (95.43(10)°) and Ru(3)−P(2)−Ru(4) obtuse (148.71(15)°).

(11) (a) Baerends, E. J.; Ellis, D. E.; Ros, P. *Chem. Phys.* **1975**, *8*, 41. (b) Baerends, E. J.; Ros, P. *Int. J. Quantum Chem.* **1978**, *S12*, 169. (c) Boerrigter, P. M.; te Velde, G.; Baerends, E. J. *Int. J. Quantum Chem.* **1988**, *33*, 87. (d) te Velde, G.; Baerends, E. J. *J. Comput. Phys.* **1992**, *99*, 84.

(12) Amsterdam Density Functional (ADF) program, version 2.3; Vrije Universiteit, Amsterdam, The Netherlands, 1997.

(13) Vosko, S. D.; Wilk, L.; Nusair, M. *Can. J. Chem.* **1990**, *58*, 1200.

(14) Blenkiron, P.; Enright, G. D.; Low, P. J.; Corrigan, J. F.; Taylor, N. J.; Chi, Y.; Saillard, J.-Y.; Carty, A. J. *Organometallics* **1998**, *17*, 2447−2458.

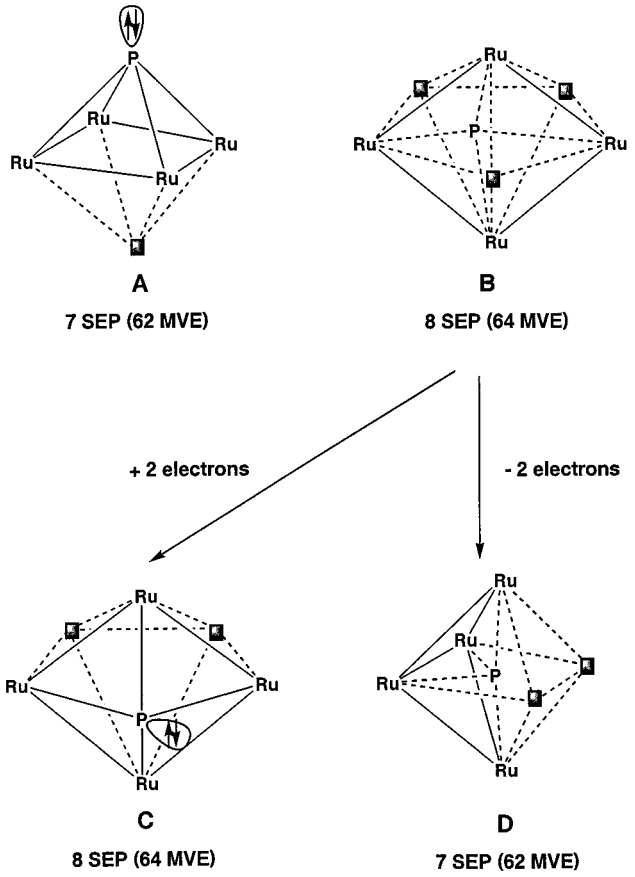

Figure 3. Possible idealized representations of $Ru_4(CO)_{12}(\mu\text{-}PF_2)(\mu_4\text{-}P)$ (**A** and **B**) and of their reduced (**C**) and oxidized (**D**) forms.

In describing the skeletal framework and the electron count of $Ru_4(CO)_{12}(\mu\text{-}PF_2)(\mu_4\text{-}P)$, we make the reasonable assumption that the $\mu\text{-}PF_2$ group behaves as a three-electron bridging ligand and is not a part of the core skeleton. The bare phosphorus atom P(2), on the other hand, is part of an Ru_4P skeleton in which the position of P(2) is intermediate between that of a vertex of a fundamental deltahedron and that of an exposed main-group atom. These two extreme views are sketched in structures **A** and **B** of Figure 3. Situation **A** describes a mixed transition-metal/main-group *nido* species in which the bare phosphorus atom provides the cluster skeleton with three electrons, an exo-skeletal lone pair being retained on this atom. This leads to an electron count of 7 SEPs, i.e. 62 metal valence electrons (MVE),[15] in full agreement with the PSEP rules. Situation **B** corresponds to a *hypho* species based on a pentagonal-bipyramidal deltahedron. In this situation, the exposed phosphorus atom provides the cluster skeleton with all 5 of its valence electrons, leading to the 8-SEP (or 64-MVE) count. Therefore, **B** also obeys the PSEP rules. We note that **B** also satisfies the 18-electron rule, 64 MVE being the expected count for a tetranuclear species in which 4 localized Ru−Ru bonds are present. It is likely that the mismatch between the atomic radii of Ru and P and/or the pinch effect of the $\mu\text{-}PF_2$ ligand prevent $Ru_4(CO)_{12}(\mu\text{-}PF_2)(\mu_4\text{-}P)$ from adopting one of the ideal geometries **A** and **B**. The question which arises then is this: which situation **A** or **B** more closely describes $Ru_4(CO)_{12}(\mu\text{-}PF_2)(\mu_4\text{-}P)$? In other words, how many electrons (3 or 5) are given by P(2) to the metal atoms? To provide a clear answer to this question and to understand the bonding and stability of $Ru_4(CO)_{12}(\mu\text{-}PF_2)(\mu_4\text{-}P)$, DFT calculations have been carried out on $Ru_4(CO)_{12}(\mu\text{-}PF_2)(\mu_4\text{-}P)$ and on a series of related compounds.

(15) All the bonding and nonbonding peripheral electrons which lie in the environment of the metal atoms have to be added to the skeletal electron number in order to reach the MVE count.

Theoretical Investigation of the $[Ru_4(CO)_{12}(\mu\text{-}PF_2)(\mu_4\text{-}P)]^q$ ($q = 2-, 0, 2+$) Series. The molecular structure of $Ru_4(CO)_{12}(\mu\text{-}PF_2)(\mu_4\text{-}P)$ has been optimized assuming C_{2v} symmetry. This is shown in Figure 4, and the major structural parameters are given in Table 3, together with the corresponding average experimental values. To avoid confusion, the same atom labeling as that used in the X-ray structure has been chosen. The agreement between the theoretical and experimental structures is very good. In particular, the optimized and X-ray values of Ru(1)−Ru(2)−Ru(3)−Ru(4), the butterfly angle, and the P(2) bond angles are almost the same. This gives confidence in the validity of the theoretical calculations. The computed HOMO−LUMO gap is large (2.35 eV), in agreement with the diamagnetism, color, and stability of $Ru_4(CO)_{12}(\mu\text{-}PF_2)(\mu_4\text{-}P)$.

A simple way of checking whether the phosphorus atom in $Ru_4(CO)_{12}(\mu\text{-}PF_2)(\mu_4\text{-}P)$ acts as a 3-electron or a 5-electron donor to the tetranuclear metal unit is to change the electron count of the cluster. Assuming that $Ru_4(CO)_{12}(\mu\text{-}PF_2)(\mu_4\text{-}P)$ is best described by the 62-MVE structure **A** in Figure 3, i.e., P is a 3-electron donor, the addition of two extra electrons to the cluster is expected to break a skeletal metal−metal or metal−ligand bond. On the other hand, if P is a 5-electron donor (64-MVE idealized structure **B** in Figure 3), the addition of 2 extra electrons is expected to shift the exposed P(2) atom toward a vertex of the fundamental deltahedron, which is a pentagonal bipyramid.[8] A possible idealized *nido* structure is sketched in **C** of Figure 3**.** In this situation, an exo-skeletal lone pair is created on P(2), which now acts as a 3-electron donor so that the 64-MVE (8-SEP) count is maintained upon reduction. Conversely, the removal of 2 electrons from structure **A** is likely to lead to a 60-MVE (6-SEP) *closo* Ru_4P trigonal bipyramid exhibiting a pyramidalized phophorus atom, whereas removing two electrons from structure **B** should not modify the coordination mode of P, since all of its orbitals are involved in the bonding. The expected effect is the creation of a Ru−Ru bond, as exemplified by the 62-MVE (7-SEP) idealized structure sketched in **D** of Figure 3.

Our DFT calculations show that the optimized geometries of $[Ru_4(CO)_{12}(\mu\text{-}PF_2)(\mu_4\text{-}P)]^{2-}$ and $[Ru_4(CO)_{12}(\mu\text{-}PF_2)(\mu_4\text{-}P)]^{2+}$ can be idealized by structures **C** and **D**, respectively, indicating that $Ru_4(CO)_{12}(\mu\text{-}PF_2)(\mu_4\text{-}P)$ should be better considered as being a 64-MVE species best described by structure **B** (see Figure 4 and Table 3). The 2-electron reduction of $Ru_4(CO)_{12}(\mu\text{-}PF_2)(\mu_4\text{-}P)$ induces significant pyramidalization of P(2) associated with an increase of the Ru_4 butterfly angle. Also the Ru−P bonds are weakened, whereas the 4 Ru−Ru bonds are slightly shortened. The 2-electron oxidation of $Ru_4(CO)_{12}(\mu\text{-}PF_2)(\mu_4\text{-}P)$ induces the formation of a bond along the Ru(1)−Ru(2) butterfly hinge. This bond is

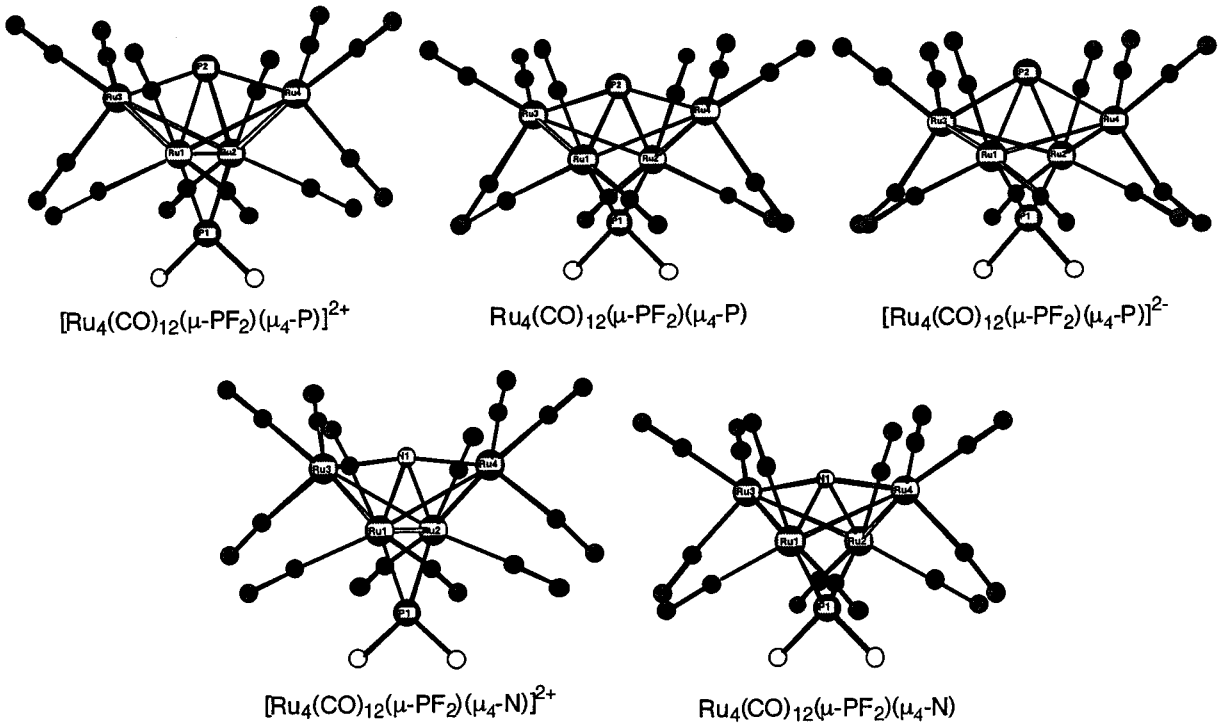

Figure 4. DFT-optimized molecular structures of the $[Ru_4(CO)_{12}(\mu\text{-}PF_2)(\mu_4\text{-}P)]^q$ ($q = 2-$, 0, 2+) and $[Ru_4(CO)_{12}(\mu\text{-}PF_2)(\mu_4\text{-}N)]^q$ ($q = 0$, 2+) series.

Table 3. Major DFT Results Computed for the Series $[Ru_4(CO)_{12}(\mu\text{-}PF_2)(\mu_4\text{-}E)]^q$ (E = N, P; $q = 2+$, 0, 2−)[a]

	$[Ru_4(CO)_{12}(\mu\text{-}PF_2)(\mu_4\text{-}P)]^q$ (C_{2v})			$[Ru_4(CO)_{12}(\mu\text{-}PF_2)(\mu_4\text{-}N)]^q$ (C_{2v})	
	$q = 2+$	$q = 0$	$q = 2-$	$q = 2+$	$q = 0$
Ru(1)−Ru(3) (Å)	2.950	3.009 (2.978)	2.952	2.803	2.841
Ru(1)···Ru(2) (Å)	2.861	3.662 (3.634)	3.700	2.773	3.571
Ru(1)−E (Å)	2.409	2.474 (2.456)	2.644	2.110	2.249
Ru(3)−E (Å)	2.319	2.223 (2.188)	2.433	2.020	1.934
Ru(1)−P(1) (Å)	2.304	2.322 (2.277)	2.320	2.309	2.319
Ru(3)−P(1) (Å)	3.823	3.281 (3.219)	3.071	3.798	3.215
P(1)−F (Å)	1.569	1.602 (1.598)	1.648	1.565	1.613
Ru(1)−E(2)−Ru(2) (deg)	72.9	94.5 (95.4)	88.8	82.1	105.1
Ru(3)−E(2)−Ru(4) (deg)	148.1	148.4 (148.7)	125.7	167.9	164.2
Ru_4 butterfly dihedral angle (deg)	119.5	127.3 (126.4)	140.4	111.1	120.2

[a] Averaged experimental values of $[Ru_4(CO)_{12}(\mu\text{-}PF_2)(\mu_4\text{-}P)]$ are given in parentheses.

shorter than the four other Ru−Ru bonds (2.861 vs 2.950 Å). The butterfly angle is decreased, while the Ru(3)−P(2)−Ru(4) angle remains almost constant.

Comparison of the $[Ru_4(CO)_{12}(\mu\text{-}PF_2)(\mu_4\text{-}P)]^{2+/0}$ Clusters with Reported Isoelectronic Nitride and Carbide Species. It is noteworthy that the $[Ru_4(CO)_{12}(\mu\text{-}PF_2)(\mu_4\text{-}P)]^{2+}$ 62-MVE (7-SEP) hypothetical cation is isoelectronic with members of the $[M_4(CO)_{12}(\mu_4\text{-}N)]^-$ (M = Fe, Ru, Os) series[16] and with other related nitride[17] and carbide[6,18] tetranuclear species. All of these compounds adopt the ideal geometry exemplified by $[Fe_4(CO)_{12}(\mu_4\text{-}C)]^{2-}$ in Figure 1, i.e. with an almost linear M(3)−E−M(4) (E = N, C) arrangement (179, 176, and 173° in the case of M = Fe, Ru, Os, respectively[16]). With a corresponding value of 148°, the optimized geometry of $[Ru_4(CO)_{12}(\mu_2\text{-}PF_2)(\mu_4\text{-}P)]^{2+}$ is much farther from the ideal structure of Figure 1. It also has a somewhat larger butterfly dihedral angle (119 vs 102−105°[16]). To understand these differences, which may result either from the different sizes of C, N, and P or from the presence of a bridging PF_2 ligand in $[Ru_4(CO)_{12}(\mu\text{-}PF_2)(\mu_4\text{-}P)]^{2+}$, we have carried out calculations on the 62-MVE model series $[M_4(CO)_{12}(\mu_4\text{-}E)]^-$ (M = Fe, Ru; E = N, P). The M_4E cores of the optimized geometries are shown in Figure 5, and some metrical data are given in Table 3, together with the corresponding averaged experimental values. The DFT structures of the nitride compounds $[Fe_4(CO)_{12}(\mu_4\text{-}N)]^-$ and $[Ru_4(CO)_{12}(\mu_4\text{-}N)]^-$ are in good agreement with the reported crystal structures.[16a,b] Changing N into P in these clusters results in a pyramidalization of this atom (M(3)−E−

(16) (a) Fjare, D. J.; Gladfelter, W. L. *J. Am. Chem. Soc.* **1981**, *103*, 1572. (b) Harris, S.; Blohm, M. L.; Gladfelter, W. L. *Inorg. Chem.* **1989**, *28*, 2290. (c) Collins, M. A.; Johnson, B. F. G.; Lewis, J.; Mace, J.; Morris, J.; McPartlin, N.; Nelson, W. J. H.; Puga, J.; Raithby, P. R. *J. Chem. Soc., Chem. Commun.* **1983**, *689*.

(17) (a) Tachikawa, M.; Stein, J.; Muetterties, E. L.; Teller, R. G.; Beno, M. A.; Gebert, E.; Williams, J. M. *J. Am. Chem. Soc.* **1980**, *102*, 6648. (b) Braga, D.; Johnson, B. F. G.; Lewis, J.; Mace, J. M.; McPartlin, M.; Puga, J.; Nelson, W. J. H.; Raithby, P. R.; Whitmire, K. H. *J. Chem. Soc., Chem. Commun.* **1982**, 1081. (c) Blohm, M. L.; Fjare, D. E.; Gladfelter, W. L. *J. Am. Chem. Soc.* **1986**, *108*, 2301. (d) Fjare, D. E.; Gladfelter, W. L. *J. Am. Chem. Soc.* **1984**, *106*, 4799.

(18) (a) Bradley, J. S.; Ansell, G. B.; Leonowicz, M. E.; Hill, E. W. *J. Am. Chem. Soc.* **1981**, *103*, 4968. (b) Hriljac, J. A.; Swepston, P. N.; Shriver, D. F. *Organometallics* **1985**, *4*, 158. (c) Chi, Y.; Chuang, S.-H.; Chen, B.-F.; Peng, S.-M.; Lee, G.-H. *J. Chem. Soc., Dalton Trans.* **1990**, 3033.

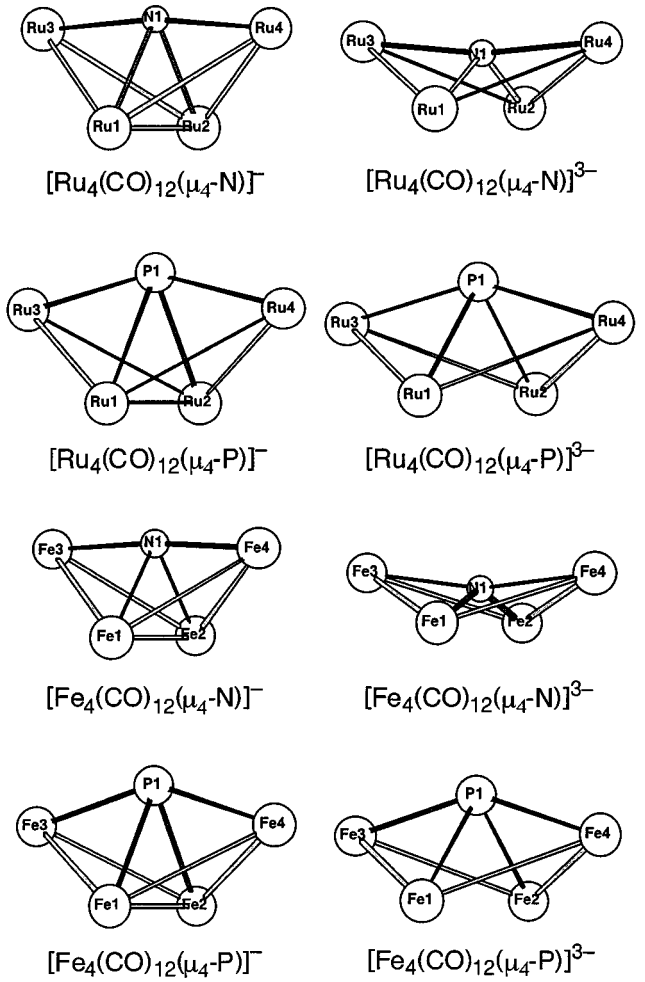

Figure 5. M_4E cores of the DFT-optimized geometries of the $[M_4(CO)_{12}(\mu_4\text{-}E)]^q$ (M = Fe, Ru; E = N, P; $q = 1-, 3-$) series.

M(4) = 147 and 152° for M = Fe, Ru, respectively). Thus, it is clear that, even in the case of second-row metals, the size of the exposed phosphorus atom requires some pyramidalization in these 62-MVE clusters.

Two tetranuclear nitride compounds isoelectronic with $Ru_4(CO)_{12}(\mu\text{-}PF_2)(\mu_4\text{-}P)$ have also been reported, namely $Ru_4(CO)_{12}(\mu\text{-}NO)(\mu_4\text{-}N)$ and $Ru_4(CO)_{12}(\mu\text{-}NCO)(\mu_4\text{-}N)$.[19] The molecular structures of these 64-MVE clusters derive from that of the 62-MVE $[M_4(CO)_{12}(\mu_4\text{-}N)]^-$ series by opening of the M(1)−M(2) butterfly hinge, with nonbonding distances of ∼3.2 Å bridged by the NO or NCO ligand. The butterfly angles are ∼110°, and the Ru(3)−N−Ru(4) arrangement is maintained almost linear (∼174°). DFT calculations on the (unbridged) 64-MVE $[M_4(CO)_{12}(\mu_4\text{-}E)]^{3-}$ (M = Fe, Ru, E = N, P) models assuming C_{2v} symmetry yielded structures derived from the $[M_4(CO)_{12}(\mu_4\text{-}E)]^-$ series by simply opening the M(1)−M(2) bond. These M_4E cores are shown in Figure 5. As for the neutral series, the exposed P atoms exhibit some pyramidalization, whereas the exposed N atoms do not (see Figure 5 and Table 4). Rather, the $[M_4(CO)_{12}(\mu_4\text{-}N)]^{3-}$ models exhibit M(3)−N−M(4) angles which are larger than 180°; that is, the nitrogen atom is slightly shifted toward the middle of the M(1)···M(2) vector, lying now in the groove of the M_4 butterfly. Such a peculiarity is also present in the X-ray structure of the 64-MVE carbide cluster $[Re_4(CO)_{15}I(\mu_4\text{-}N)]^-$, in which all of the carbonyl and iodine ligands are terminal.[20]

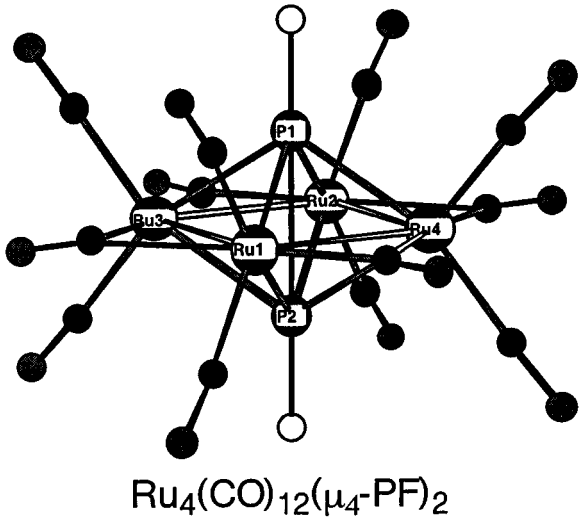

Figure 6. Optimized geometry of the hypothetical *closo*-$Ru_4(CO)_{12}(\mu_4\text{-}PF)_2$ isomer of $Ru_4(CO)_{12}(\mu\text{-}PF_2)(\mu_4\text{-}P)$.

These results show clearly that it is mainly a size effect which causes phosphorus to pyramidalize, in contrast to nitrogen. It turns out, however, that the presence of the PF_2 bridging ligand also has some influence on the pyramidalization of P(2) in the title compound, as shown by the optimized geometries of the 62-MVE and 64-MVE nitride models $[Ru_4(CO)_{12}(\mu\text{-}PF_2)(\mu_4\text{-}N)]^{2+/0}$ (see Figure 4 and Table 3).[21] These nitride species have molecular structures similar to those of their phosphide analogues, including some pyramidalization (although much less pronounced) of the exposed atom.

Alternative Phosphinidene Isomers. Because a large number of $M_4L_n(\mu_4\text{-}PR)_2$ species exist having a *closo* octahedral M_4P_2 core, it is pertinent to ask whether $Ru_4(CO)_{12}(\mu\text{-}PF_2)(\mu_4\text{-}P)$ could also exist in the form of $Ru_4(CO)_{12}(\mu_4\text{-}PF)_2$ sketched in Figure 6. It has been

Table 4. Major DFT Results Computed for the Series $[M_4(CO)_{12}(\mu_4\text{-}E)]^{n-}$(M = Ru, Fe; E = N, P; $n = 1, 3$)[a]

	$[Ru_4(CO)_{12}(\mu_4\text{-}E)]^{n-}$ (C_{2v})				$[Fe_4(CO)_{12}(\mu_4\text{-}E)]^{n-}$ (C_{2v})			
	$n = 1$		$n = 3$		$n = 1$		$n = 3$	
	E = N	E = P	E = N	E = P	E = N	E = P	E = N	E = P
M(1)−M(3) (Å)	2.793 (2.787)	2.958	2.947	3.049	2.548 (2.604)	2.691	2.648	2.804
M(1)−M(2) (Å)	2.681 (2.672)	2.773	3.989	3.450	2.498 (2.512)	2.570	3.624	3.181
M(1)−E (Å)	2.100 (2.069)	2.394	2.165	2.418	1.879 (1.900)	2.218	1.881	2.235
M(3)−E (Å)	1.971 (1.920)	2.271	1.922	2.346	1.782 (1.771)	2.119	1.799	2.179
M(1)−E−M(2) (deg)	79.3 (80.5)	70.8	134.3	91.0	83.4 (82.8)	70.8	149.0	90.7
M(3)−E−M(4) (deg)	171.1 (176.2)	152.1	190.9	150.1	175.1 (179.0)	147.1	195.1	148.0
M_4 butterfly dihedral angle (deg)	106.7 (103.4)	115.0	123.7	128.7	106.6 (101.8)	118.6	135.0	130.3

[a] Available average experimental values of $[M_4(CO)_{12}(\mu_4\text{-}N)]^-$ (M = Ru, Fe)[16a,b] are given in parentheses.

shown[22] that two favored closed-shell electron counts are possible for octahedral $M_4L_n(\mu_4\text{-}PR)_2$ architectures, either 62 MVEs (7 SEPs) or 64 MVEs (8 SEPs). With M = Ru, the 64-MVE count is unlikely.[9a,22b] This may explain why the alternative $Ru_4(CO)_{12}(\mu_4\text{-}PF)_2$ octahedral architecture is not observed. As a matter of fact, DFT geometry optimization of this hypothetical isomer was found to be 0.21 eV less stable than the $Ru_4(CO)_{12}(\mu\text{-}PF_2)(\mu_4\text{-}P)$ structure. It is indeed interesting that our synthetic work has revealed no evidence of an isomer of $Ru_4(CO)_{12}(\mu\text{-}PF_2)(\mu_4\text{-}P)$. Conversely, calculations on the 62-MVE $[Ru_4(CO)_{12}(\mu_4\text{-}PF)_2]^{2+}$ cation (Table 3) found this octahedral arrangement to be more stable than the $[Ru_4(CO)_{12}(\mu\text{-}PF_2)(\mu_4\text{-}P)]^{2+}$ structure by 0.88 eV.

Acknowledgment. Computing facilities were provided by the Centre de Ressources Informatiques (CRI) of Rennes and the Institut de Développement et de Ressources en Informatique Scientifique du Centre National de la Recherche Scientifique (IDRIS-CNRS). Financial support (to A.J.C.) was provided by the National Research Council of Canada and the Natural Sciences and Engineering Research Council of Canada.

Supporting Information Available: Tables of X-ray crystallographic information in CIF format for $Ru_4(CO)_{12}(\mu\text{-}PF_2)(\mu_4\text{-}P)$. This material is available free of charge via the Internet at http://pubs.acs.org.

OM010352U

(19) Attard, J. P.; Johnson, B. F. G.; Lewis, J.; Mace, J. M.; Raithby, P. R. *J. Chem. Soc., Chem. Commun.* **1985**, 1526.

(20) Beringhelli, T.; Ciani, G.; D'Alfonso, G.; Sironi, A.; Freni, M. *J. Chem. Soc., Chem. Commun.* **1985**, 978.

(21) Exploratory calculations suggest that the reduced species $[Ru_4(CO)_{12}(\mu\text{-}PF_2)(\mu_4\text{-}N)]^{2-}$ is likely to be unstable.

(22) (a) Halet, J.-F.; Hoffmann, R.; Saillard, J.-Y. *Inorg. Chem.* **1985**, *25*, 1695. (b) Halet, J.-F.; Saillard, J.-Y. *New J. Chem.* **1987**, *11*, 315.